

IMPROVED DETERMINATION OF INCLUSIVE ELECTROMAGNETIC
DECAY RATIOS OF HEAVY QUARKONIUM FROM QCD**Yuichiro Kiyo^a, Antonio Pineda^b and Adrian Signer^c**^a *Theory Center, KEK, Tsukuba, Ibaraki 305-0801, Japan*^b *Grup de Física Teòrica and IFAE, Universitat Autònoma de Barcelona,
E-08193 Bellaterra, Barcelona, Spain*^c *Institute for Particle Physics Phenomenology
Durham, DH1 3LE, England***Abstract**

We consider a different power counting in potential NRQCD by incorporating the static potential exactly in the leading order Hamiltonian. We compute the leading relativistic corrections to the inclusive electromagnetic decay ratios in this new scheme. The effect of this new power counting is found to be large (even for top). We produce an updated value for the η_b decay to two photons. This scheme also brings consistency between the weak coupling computation and the experimental value of the charmonium decay ratio.

1 Introduction

The determination of heavy quarkonium properties from QCD has always been a major objective in high energy physics. In this respect, the development of effective field theories (EFT) directly derived from QCD like NRQCD [1] or pNRQCD [2] (for a review see Ref. [3]) has opened the door to model independent determinations of heavy quarkonium properties. Instrumental in this development is the fact that heavy quarkonium systems can be considered to be non-relativistic (NR). They are then characterized by, at least, three widely separated scales: hard (the mass m , of the heavy quarks), soft (the relative momentum $|\mathbf{p}| \sim mv \ll m$, of the heavy-quark–antiquark pair in the center of mass frame), and ultrasoft (the typical kinetic energy $E \sim mv^2$ of the heavy quark in the bound state system).

In this paper we focus on pNRQCD. This EFT takes full advantage of the hierarchy of scales that appear in the system,

$$m \gg mv \gg mv^2 \dots, \quad (1)$$

and makes a systematic and natural connection between quantum field theory and the Schrödinger equation. Schematically the EFT takes the form

$$\left. \begin{aligned} &\left(i\partial_0 - \frac{\mathbf{p}^2}{m} - V_s^{(0)}(r)\right) \Phi(\mathbf{r}) = 0 \\ &+ \text{corrections to the potential} \\ &+ \text{interactions with other low-energy degrees of freedom} \end{aligned} \right\} \text{pNRQCD}$$

where $V_s^{(0)}(r)$ is the static potential and $\Phi(\mathbf{r})$ is the $Q\bar{Q}$ wave function.

A major issue to be settled is to decide upon the precise form of $V_s^{(0)}(r)$, in particular whether one works in the weak or strong coupling regime and how to treat subleading terms. In the strict weak coupling regime one could approximate the static potential by the Coulomb potential $V_s^{(0)}(r) \simeq V_C = -C_F \alpha_s/r$ and include higher-order terms perturbatively. There seems to be growing consensus that the weak coupling regime appears to work properly for $t\bar{t}$ production near threshold, the bottomonium ground state mass, and bottomonium sum rules (for a recent discussion on this issue see [4]). One would then expect that other properties of the bottomonium ground state like the hyperfine splitting or electromagnetic decay widths could be described as well by the weak coupling version of pNRQCD. However, in this case the situation is not that clear. There has been a precise determination of the bottomonium ground state hyperfine splitting using the renormalization group in pNRQCD [5]. Nevertheless, the predicted value does not agree well with the recently obtained experimental number [6, 7]. Therefore the situation remains unsettled. For the inclusive electromagnetic decays the

convergence is not very good [8]. Even for top, higher-order corrections to the normalization appear to be sizable [8, 9, 10, 11].

In principle, the novel feature of these observables (maybe more so for the decays) compared to the heavy quarkonium ground state mass is a bigger sensitivity to the value of the wave function at the origin and to its relativistic corrections. Note that in this case the relativistic corrections are divergent and their divergences have to be absorbed by the matching coefficients of the effective theory: potentials and current matching coefficients. If one considers the decay ratio, the dependence on the wave function associated to the static potential drops out and only the relativistic correction survives. This makes the decay ratio the cleanest possible place on which to quantify the importance of the relativistic corrections to the wave function.

In Ref. [12] the decay ratios have been computed with NNLL accuracy, accounting for the resummation of logarithms. The scale dependence has greatly improved over fixed-order computations and the result is much more stable. The convergence could be classified as good for the top case, reasonable for the bottom, and not good for the charm, although in all three cases the scale dependence of the theoretical result was quite small. For the case of the charm there is experimental data available, and the agreement with experiment deteriorates when higher order corrections are introduced. On the other hand there exists a nice analysis for charmonium in Ref. [13], where they consider a potential model (a Cornell-like one, yet compatible with perturbation theory at short distances, since it is coulomb-like in this regime) for the bound state dynamics, but a tree-level perturbative potential for the spin-dependence. They also correctly performed the matching in the ultraviolet with QCD along the lines of what would be pNRQCD in the strong coupling regime¹. Their net result was that they were able to obtain consistency with experiment albeit with large errors. Unfortunately, this result suffers from model dependence. In particular, since a perturbative potential has been used for the spin-dependent potential, it would have been more consistent to treat the static potential also in a perturbative approach. In this respect, it has been shown in Refs. [14, 15, 16, 17] that, once the renormalon cancellation is taken into account, the inclusion of perturbative corrections to the static potential leads to a convergent series and that this series gets closer to the lattice values in the quenched approximation up to scales of around 1 GeV. It is then natural to ask whether the inclusion of these effects may lead to a better agreement in the case of charmonium and for sizable corrections in the case of bottomonium and $t\bar{t}$ production near threshold. Note that in this comparison between lattice and perturbation theory one has to go to high orders to get good agreement. Therefore, a computation of the relativistic correction based on the

¹Actually the whole computation would fit into the strong coupling regime of pNRQCD except for the fact that the spin-dependent potential is computed in perturbation theory.

leading order expression for the static potential, i.e. the Coulomb potential, as the one used in an strict NNLL computation, may lead to large corrections, since these corrections, as well as the wave function at the origin, could be particularly sensitive to the shape of the potential.

Therefore, in this paper we reorganize the perturbative expansion and consider the static potential exactly, whereas we treat the relativistic terms as corrections. By doing so we expect to have an effect similar to the one observed in Ref. [13]. Including also the renormalization group improved expressions, we expect to obtain results with only a modest scale dependence. The explicit computation will confirm to a large extent these expectations. We will be able to give an updated prediction for the decay of the η_b to two photons and obtain a result for the charm decay ratio compatible with experiment (though in this last case with rather large errors). Note that our computation is completely based on a weak coupling analysis derived from QCD and no non-perturbative input is introduced.

2 Decay ratio

The one-photon mediated processes are induced by the electromagnetic current j_μ , which has the following decomposition in terms of operators constructed from the non-relativistic quark and anti-quark two-component Pauli spinors ψ and χ [18]:

$$\mathbf{j} = c_v(\mu)\psi^\dagger\boldsymbol{\sigma}\chi + \frac{d_v(\mu)}{6m_q^2}\psi^\dagger\boldsymbol{\sigma}\mathbf{D}^2\chi + \dots, \quad (2)$$

where μ is the renormalization scale, \mathbf{D} is the covariant derivative, $\boldsymbol{\sigma}$ is the Pauli matrix, and the ellipsis stands for operators of higher mass dimension. The Wilson coefficients c_v and d_v represent the contributions from the hard modes and may be evaluated as a series in α_s in full QCD for free on-shell on-threshold external (anti)quark fields. We define it through

$$c_v(\mu) = \sum_{i=0}^{\infty} \left(\frac{\alpha_s(\mu)}{\pi} \right)^i c_v^{(i)}(\mu), \quad c_v^{(0)} = 1, \quad (3)$$

and similarly for other coefficients. The coefficients $c_v^{(1)}$ and $c_v^{(2)}$ have been computed in Refs. [19] and [20, 21] respectively.

The operator responsible for the two-photon S -wave processes in the non-relativistic limit is generated by the expansion of the product of two electromagnetic currents and has the following representation [18]

$$O_{\gamma\gamma} = c_{\gamma\gamma}(\mu)\psi^\dagger\chi + \frac{d_{\gamma\gamma}(\mu)}{6m_q^2}\psi^\dagger\mathbf{D}^2\chi + \dots, \quad (4)$$

which reduces to the pseudo-scalar current in the non-relativistic limit. The coefficients $c_{\gamma\gamma}^{(1)}$ and $c_{\gamma\gamma}^{(2)}$ have been computed in Refs. [22] and [23] (in semi-numerical form) respectively.

Let us define the spin ratio for the production and annihilation of heavy quarkonium \mathcal{Q} as

$$\mathcal{R}_q = \frac{\sigma(e^+e^- \rightarrow \mathcal{Q}(n^3S_1))}{\sigma(\gamma\gamma \rightarrow \mathcal{Q}(n^1S_0))} = \frac{\Gamma(\mathcal{Q}(n^3S_1) \rightarrow e^+e^-)}{\Gamma(\mathcal{Q}(n^1S_0) \rightarrow \gamma\gamma)}. \quad (5)$$

The effective theory expression for the spin ratio reads

$$\mathcal{R}_q = \frac{c_s^2(\mu)}{3Q_q^2} \frac{|\psi_n^v(0)|^2}{|\psi_n^p(0)|^2} + \mathcal{O}(\alpha_s v^2), \quad (6)$$

where Q_q is the quark electric charge, $c_s(\mu) = c_v(\mu)/c_{\gamma\gamma}(\mu)$, $\psi_n^{(v,p)}(\mathbf{r})$ are the spin triplet (vector) and spin singlet (pseudo-scalar) quarkonium wave functions with principal quantum number n . The wave functions describe the dynamics of the non-relativistic bound state and can be computed within pNRQCD. The latter is the Schrödinger-like effective theory of potential (anti)quarks whose energies scale like $m_q v^2$ and three-momenta scale like $m_q v$, and their multipole interaction to the ultrasoft gluons [24, 25, 26, 27]. The contributions of hard and soft modes in pNRQCD are represented by the perturbative and relativistic corrections to the effective Hamiltonian, which is systematically evaluated order by order in α_s and v around the leading order (LO) Coulomb approximation.

3 pNRQCD framework

As we have mentioned before, the framework we use to compute the decay ratio, and more specifically the wave function, is pNRQCD. For the purposes of our paper the full setup of pNRQCD is not needed. We will only need the static potential, $V_s^{(0)}(r)$, and the spin-dependent potential $V_{S^2,s}^{(2)}(r)$. Furthermore, we will reorganize the perturbative expansion. The static potential will be treated exactly by including it in the leading-order Hamiltonian

$$H^{(0)} \equiv -\frac{\nabla^2}{2m_r} + V_s^{(0)}(r), \quad (7)$$

where $m_r = m_1 m_2 / (m_1 + m_2)$. On the other hand, the spin-dependent potential (in $D = 1 + d = 4 - 2\epsilon$ dimensions)

$$\Delta H = \frac{V_{S^2,s}^{(2)}(\mu)}{m_1 m_2} = -\frac{4\pi C_F D_{S^2,s}^{(2)}}{d m_1 m_2} [\mathbf{S}_1^i, \mathbf{S}_1^j][\mathbf{S}_2^i, \mathbf{S}_2^j] \delta^{(d)}(\mathbf{r}) \quad (8)$$

is considered to be a perturbation to the result obtained with $H^{(0)}$. Therefore, we distinguish between an expansion in v and α_s . v has an expansion in α_s itself but this expansion does not converge quickly for these relativistic corrections. This remains so even after the inclusion of the renormalon cancellation, which has only a minor impact on the determination of the wave function. This is the reason we choose to take the static potential exactly.

As mentioned in the introduction there are different options on how precisely to treat $V_s^{(0)}$ and we will discuss in Section 6 the various options we consider. Roughly speaking we will take the static potential up to NNNLO including also the leading ultrasoft corrections. We will also need to define a scheme of renormalon subtraction. Therefore, the general form of the static potential will be

$$V_s^{(0)}(r) = V_{SD}(r) + 2\delta m_X, \quad (9)$$

where δm_X represents a residual mass that encodes the pole mass renormalon contribution and X stands for the specific renormalon subtraction scheme. We will show some specific examples in Section 6.3. In Eq. (9), V_{SD} is the short distance behavior of the static potential, which is independent of the scheme for renormalon subtraction (even if we use a non-perturbative potential). In momentum space it reads

$$\lim_{q \rightarrow \infty} \tilde{V}_s^{(0)}(q) = \tilde{V}_{SD}(q) = -\frac{4\pi C_F \tilde{\alpha}_{V_s^{(0)}}(q)}{\mathbf{q}^2}, \quad (10)$$

with $\tilde{\alpha}_{V_s^{(0)}}(q) \sim \alpha_s(\mu)$ (for the precise relation see Eq. (51)), where $\alpha_s(\mu)$ is the QCD coupling constant in the $\overline{\text{MS}}$ -scheme.

For the spin-dependent potential in momentum space we have

$$\begin{aligned} \tilde{V}_{S^2}^{(2)}(\mu) &= -\frac{4\pi C_F D_{S^2,s}^{(2)}(\mu)}{d} [\mathbf{S}_1^i, \mathbf{S}_1^j][\mathbf{S}_2^i, \mathbf{S}_2^j] \\ &= -\frac{4\pi C_F D_{S^2,s}^{(2)}(\mu)}{3} \left(\frac{3}{2} - S^2 + \epsilon \left(\frac{9}{2} - \frac{8}{3} S^2 \right) \right) + \mathcal{O}(\epsilon^2), \end{aligned} \quad (11)$$

where $\mathbf{S}_{1,2}$ is the spin operator for heavy quark and anti-quark, respectively and $D_{S^2,s}^{(2)}(\mu) = \alpha_s(\mu) + \dots$. In the second line in Eq.(11) the spin projection has been done, resulting in $S^2 \equiv 0$ and 2 for spin-singlet and spin-triplet states, respectively (this expression actually corresponds to the regularization prescription of [13] for the spin-zero states). We have to keep the term of $\mathcal{O}(\epsilon)$ because the spin-dependent potential generates $1/\epsilon$ divergences. The renormalization procedure for these $1/\epsilon$ will be discussed in the next section.

4 Wave function ratio

We now turn to the computation of

$$\frac{|\psi_n^v(0)|^2}{|\psi_n^p(0)|^2} \equiv \rho_n(\mu) \equiv 1 + \delta\rho_n(\mu), \quad (12)$$

Applying Rayleigh-Schrödinger perturbation theory to the problem we obtain

$$\psi_n^{v/p}(0) = \psi_n^{(0)}(0) - \hat{G}(E_n^{(0)}) \frac{\tilde{V}_{S^2}^{(2)}(\mu)}{m_1 m_2} \psi_n^{(0)}(0) + \mathcal{O}(\tilde{V}_{S^2}^{(2)})^2, \quad (13)$$

where $\psi_n^{(0)}(0)$ is the wave function for the LO Hamiltonian $H^{(0)}$ and $\hat{G}(E_n^{(0)})$ is the reduced Green function at $E = E_n^{(0)}$, which is defined by

$$\hat{G}(E_n^{(0)}) \equiv \sum'_m \frac{|\psi_m^{(0)}(0)|^2}{E_m^{(0)} - E_n^{(0)}} = \lim_{E \rightarrow E_n^{(0)}} \left(G(E) - \frac{|\psi_n^{(0)}(0)|^2}{E_n^{(0)} - E} \right). \quad (14)$$

The prime indicates that the sum does not include the state n and

$$G(E) = G(0, 0; E) \equiv \lim_{r \rightarrow 0} G(r, r; E) = \lim_{r \rightarrow 0} \langle \mathbf{r} | \frac{1}{H^{(0)} - E - i0} | \mathbf{r} \rangle \quad (15)$$

is the zero-distance limit of the Green function $G(r, r'; E)$, which is the solution of the Schrödinger equation

$$\left[-\frac{\nabla^2}{2m_r} + V_s^{(0)}(r) - E \right] G(r, r'; E) = \delta(\mathbf{r} - \mathbf{r}'). \quad (16)$$

The short distance behavior of the static potential $V_s^{(0)}(r) \sim 1/r$ makes $G(E)$ and, therefore, $\delta\rho_n$ divergent. Thus we will need to regularize the Green function and we will deal with two different ways to do this: dimensional regularization and finite- r regularization. We start by considering the former and will come back to finite- r regularization in the next section.

The divergences in $\delta\rho_n$ are cancelled by divergences in the Wilson coefficient $c_s^2(\mu)$. Since the latter have been computed in dimensional regularization we will need $G(E)$ in dimensional regularization as well. We denote the corresponding bare and reduced Green functions by $G^{(D)}(E) = G^{(D)}(0, 0; E)$ and $\hat{G}^{(D)}(E_n^{(0)})$ respectively. We remark that the LO wave functions (corresponding to $H^{(0)}$) are finite, thus $|\psi_n^{(0)(D)}(0)|^2 = |\psi_n^{(0)(4)}(0)|^2 \equiv |\psi_n^{(0)}(0)|^2$.

Using Eqs. (11)–(13), the bare expression of $\delta\rho_n(\mu)$ in dimensional regularization can be written as

$$\delta\rho_n^{(D)}(\mu) = -\frac{16\pi C_F}{3m_1 m_2} D_{S^2, s}^{(2)}(\mu) \left(1 + \frac{8}{3} \epsilon + \mathcal{O}(\epsilon^2) \right) \hat{G}^{(D)}(E_n^{(0)}). \quad (17)$$

In order to obtain the $\overline{\text{MS}}$ -renormalized expression of $\delta\rho_n$, we need to identify the divergences of $\hat{G}^{(D)}(E_n^{(0)})$. They are the same as those of $G^{(D)}(E)$, are independent of E , and can be computed order by order in perturbation theory, since they are related to the short distance behavior of the Green function. We thus parameterize the divergent and finite terms of $G^{(D)}(E)$ and $\hat{G}^{(D)}(E_n^{(0)})$ as

$$G^{(D)}(E) = \frac{m_r}{2\pi} \left[A_{\overline{\text{MS}}}^{(D)}(\epsilon; \mu) + B_{V_s^{(0)}}^{\overline{\text{MS}}}(E; \mu) \right], \quad (18)$$

$$\hat{G}^{(D)}(E_n^{(0)}) = \frac{m_r}{2\pi} \left[A_{\overline{\text{MS}}}^{(D)}(\epsilon; \mu) + \hat{B}_{V_s^{(0)}}^{\overline{\text{MS}}}(E_n^{(0)}; \mu) \right], \quad (19)$$

where $B_{V_s^{(0)}}^{\overline{\text{MS}}}(E; \mu)$ and $\hat{B}_{V_s^{(0)}}^{\overline{\text{MS}}}(E_n^{(0)}; \mu)$ are finite in 4 dimensions, but contain terms to all orders in α_s/v , since the bound-state dynamics needs all order resummation in α_s . As will be shown, Eq. (39), the ultraviolet divergent part can be expressed in terms of the (dimensionfull) bare coupling $g^2 \equiv 4\pi\alpha_s\mu^{2\epsilon}$ as

$$A_{\overline{\text{MS}}}^{(D)}(\epsilon; \mu) = \frac{g^2 C_F m_r}{8\pi\epsilon} \left(\frac{\mu^2 e^{\gamma_E}}{4\pi} \right)^{-2\epsilon} + \mathcal{O}(\alpha_s^2). \quad (20)$$

$A_{\overline{\text{MS}}}^{(D)}$ will be removed by renormalization. This has to be done consistently with the calculation of other parts order by order in the expansion in α_s (in our case $\overline{\text{MS}}$). The divergences are then absorbed in c_s and we can write

$$\delta\rho_n^{\overline{\text{MS}}}(\mu) = -\frac{8m_r C_F}{3m_1 m_2} D_{S^2, s}^{(2)}(\mu) \left(\hat{B}_{V_s^{(0)}}^{\overline{\text{MS}}}(E_n^{(0)}; \mu) + \frac{4}{3} m_r C_F \alpha_s + \mathcal{O}(\alpha_s^2) \right). \quad (21)$$

This will have to be combined with the $\overline{\text{MS}}$ subtracted matching coefficient $c_s^2(\mu)$ in Eq. (6) to obtain the decay ratio.

5 Green Function in position space

The main goal of the present paper is to compute $\hat{G}^{(D)}(E_n^{(0)})$ or, equivalently, $\hat{B}_{V_s^{(0)}}^{\overline{\text{MS}}}(E_n^{(0)}; \mu)$, with the effect of the static potential included exactly. This calls for a numerical evaluation of the Green function rather than pursuing an analytic approach. Numerical calculations are most conveniently performed in coordinate space. It is here where finite- r regularization comes into play. In Section 5.1 we will discuss this regularization and in Section 5.2 we show how to convert the Green function obtained in finite- r regularization by matching into the one in dimensional regularization.

5.1 Regularization of the Green function in position space

The zero-distance Green function with finite- r regularization is simply defined as $G^{(r)}(E) \equiv G(r_0, r_0; E)$, where $r_0 \ll 1/(m\alpha_s)$. In order to compute it, we

first have to describe how to obtain a numerical solution for the Green function $G(r, r'; E)$ in general, given the static potential $V_s^{(0)}(r)$. Actually the whole procedure holds valid for a generic potential (not unbounded from below at long distances) that has the correct, perturbative, short distance limit². According to Eq. (9) renormalon associated affects are power suppressed. Therefore, they will not affect properties associated to the $r \rightarrow 0$ limit of the potential.

For the class of potentials described above, the Green function $G(r, r'; E)$ can be constructed from the two independent solutions $u_{<}(r), u_{>}(r)$ of the homogeneous Schrödinger equation (our approach follows Ref. [28], see also Ref. [29])

$$\left[\frac{d^2}{dr^2} + 2m_r (E - V_s^{(0)}(r)) \right] u(r) = 0. \quad (22)$$

Here $u(r)$ represents $u_{<}(r)$ or $u_{>}(r')$, which are the solutions to Eq. (22) that are regular for $r \rightarrow 0$ and $r' \rightarrow \infty$ respectively. The angular-momentum term is dropped in the Schrödinger equation assuming S-wave contribution because the limit $r, r' \rightarrow 0$ is taken later. The Green function is written as

$$G(r, r'; E) = \left(\frac{m_r}{2\pi} \right) \frac{u_{<}(r)}{r} \frac{u_{>}(r')}{r'} \quad \text{for } r < r'. \quad (23)$$

The numerical solution at finite r is obtained by solving the Schrödinger equation with boundary conditions at short distances. To this end we prepare two independent solutions $u_0(r)$ and $u_1(r)$ that are defined by the following initial conditions: For $u_1(r)$, which we will call the regular solution we set

$$u_1(0) = 0 \quad \text{and} \quad u_1'(0) = 1 \quad (24)$$

so that

$$u_1(r) = r + \mathcal{O}(r^2). \quad (25)$$

This completely fixes $u_1(r)$.

For the non-regular solution, $u_0(r)$, we can not work this way. Whereas we can still take $u_0(0) = 1$, we can not define $u_0'(0)$, as it becomes singular. Therefore, we first define u_0' for small values of r in the following way

$$u_0'(r) = C_0(r_c) + 2m_r \int_{r_c}^r dr' V_{SD}(r') + \mathcal{O}(r), \quad (26)$$

where $C_0(r_c)$ is an integration constant. Note that $r_c > 0$ acts as a cutoff to avoid the denominator-zero of $V_{SD}(r')$. The total solution then reads (at short distances)

$$u_0(r) = 1 + C_0(r_c) r + 2m_r \int_0^r dr' \int_{r_c}^{r'} dr'' V_{SD}(r'') + \mathcal{O}(r^2). \quad (27)$$

²This opens the possibility of using the same formalism for pNRQCD in the strong coupling regime but then we should also consider a non-perturbative potential in Eq. (8), albeit with the correct short distance limit.

This expression can be rewritten as

$$u_0(r) = 1 + C_0(r_c) r + 2m_r r \left\{ \int_{r_c}^r dr' V_{SD}(r') - \int_0^r dr' \frac{r' V_{SD}(r')}{r} \right\} + \mathcal{O}(r^2). \quad (28)$$

The derivatives $u'_{0,1}(r)$ and $u_{0,1}(r)$ at small r are used as boundary conditions to solve differential equations by, for instance, the Runge-Kutta method. For later convenience we take $r_c = 1/(\mu e^{\gamma_E})$ and fix

$$C_0(r_c) = -\frac{2m_r}{r_c} \int_0^{r_c} dr' \int_{r_c}^{r'} dr'' V_{SD}(r'') = 2m_r \int_0^{r_c} dr' \frac{r' V_{SD}(r')}{r_c}. \quad (29)$$

With this choice the $\mathcal{O}(r)$ term of Eq. (28) for u_0 is a function of $\ln(\mu e^{\gamma_E} r)$ with no log-independent terms

$$u_0(r) = 1 + 2m_r r \sum_{n=1}^{\infty} v_n \ln^n(\mu e^{\gamma_E} r) + \mathcal{O}(r^2). \quad (30)$$

The coefficients v_n , which can be written as an expansion in powers of $\alpha_s(\mu)$, only depend on the coefficients a_n of V_{SD} (see Eq. (52)), i.e. only on the pure short distance behavior of the static potential. This choice will turn out to be very convenient for the conversion to dimensional regularization, but the final result for $G(r, r; E)$ does not depend on this choice.

From the two solutions $u_0(r)$ and $u_1(r)$ we can construct $u_{>}(r)$ and $u_{<}(r)$ as follows: First the solution at short distance $u_{<}(r)$ is identified as

$$u_{<}(r) = u_1(r), \quad (31)$$

because $\lim_{r \rightarrow 0} u_1(r) = 0$. The other solution which satisfies $\lim_{r \rightarrow \infty} u_{>}(r) = 0$ is given by

$$u_{>}(r) = u_0(r) + B_{V_s^{(0)}}^{(r)}(E) u_1(r), \quad (32)$$

$$B_{V_s^{(0)}}^{(r)}(E) = -\lim_{r \rightarrow \infty} \{ u_0(r)/u_1(r) \}. \quad (33)$$

From the boundary conditions of u_0 and u_1 it follows that we can mix a u_1 -component into $u_0(r)$. However, the precise choice of $u_0(r)$ does not affect $u_{>}(r)$ because of the invariance under $u_0(r) \rightarrow u_0(r) + \kappa u_1(r)$ with κ being an arbitrary constant. The zero-distance Green function with finite- r regularization is then obtained as

$$G^{(r)}(E) = \frac{m_r}{2\pi} \left[A^{(r)}(r_0; \mu) + B_{V_s^{(0)}}^{(r)}(E; \mu) \right], \quad (34)$$

$$A^{(r)}(r_0; \mu) = \frac{u_0(r_0)}{r_0} = \frac{1}{r_0} - 2m_r C_F \alpha_s \ln(\mu e^{\gamma_E} r_0) + \mathcal{O}(\alpha_s^2), \quad (35)$$

where the last equality is a good approximation for $\mu e^{\gamma_E} r_0 \sim 1$. $A^{(r)}(r_0; \mu)$ encodes the divergence of $G^{(r)}(E)$ and plays the role of the $1/\epsilon$ pole of $G^{(D)}(E)$. It is energy independent because it is related to the overall divergence of the Green function. Nevertheless, note that according to Eq. (34) we define $B_{V_s^{(0)}}^{(r)}(E; \mu)$ by subtracting exactly $u_0(r_0)/r_0$, which, depending on the potential, will include terms with arbitrary powers of α_s . $B^{(r)}(E; \mu)$ is computed numerically by solving the Schrödinger equation and is independent of the regulator r_0 . Note however that it is scheme dependent, i.e. it depends on the specific condition we use for $u'_0(r_0)$. This dependence cancels between $A^{(r)}$ and $B_{V_s^{(0)}}^{(r)}$ such that $G^{(r)}(E)$ is independent of the specific choice for $u'_0(r_0)$. In analogy to Eq. (19) we also define

$$\hat{G}^{(r)}(E_n^{(0)}) = \frac{m_r}{2\pi} \left[A^{(r)}(r_0; \mu) + \hat{B}_{V_s^{(0)}}^{(r)}(E_n^{(0)}; \mu) \right]. \quad (36)$$

Finally we remark that $B_{V_s^{(0)}}^{(r)}$ is independent of the renormalon subtraction scheme used, since $\hat{G}^{(r)}(E_n^{(0)})$ and $A^{(r)}(r_0; \mu)$ are; the latter by the definition used in this paper.

5.2 Conversion to the $\overline{\text{MS}}$ scheme

Once we have the zero-distance Green function $G^{(r)}(E) \equiv G(r_0, r_0; E)$, where $r_0 \ll 1/(m\alpha_s)$, or more precisely $B_{V_s^{(0)}}^{(r)}$, we have to convert the result by matching into the one in dimensional regularization $B_{V_s^{(0)}}^{\overline{\text{MS}}}$, in order to be able to use Eq. (21). We define the difference

$$c_r^{\overline{\text{MS}}} = B_{V_s^{(0)}}^{\overline{\text{MS}}}(E; \mu) - B_{V_s^{(0)}}^{(r)}(E; \mu) = \hat{B}_{V_s^{(0)}}^{\overline{\text{MS}}}(E_n^{(0)}; \mu) - \hat{B}_{V_s^{(0)}}^{(r)}(E_n^{(0)}; \mu). \quad (37)$$

This difference between the schemes can be accounted for by a finite (r_0 and ϵ independent) constant. We also use the fact that the ultraviolet divergent term of the Green function is energy independent. This means that $c_r^{\overline{\text{MS}}}$ is energy independent and its perturbative expansion is short distance dominated and can be computed order by order in α_s .

Note that $c_r^{\overline{\text{MS}}}$ does not depend on the long distance behavior of $V_s^{(0)}$, only on its short distance behavior, which is universal and dictated by perturbation theory, i.e. by Eq. (10). In particular, the result is independent of the pole mass renormalon. Therefore, the value obtained for $c_r^{\overline{\text{MS}}}$ holds true for a general potential (not unbounded from below at long distances) that has the correct short distance limit.

Considering the lowest order approximation of the static potential, the Coulomb

potential

$$V_s^{(0)} \simeq V_C = -C_F \frac{\alpha_s(\mu)}{r}. \quad (38)$$

the exact solution for this potential, the Coulomb Green function, is known in dimensional regularization and can be expressed in terms of $\lambda \equiv C_F \alpha_s / \sqrt{-2E/m_r}$ as

$$G_c^{(D)}(E) = \frac{g^2 C_F m_r^2}{4\pi^2} \left(\frac{-8m_r E}{4\pi e^{-\gamma_E}} \right)^{-2\epsilon} \left[\frac{1}{4\epsilon} - \frac{1}{2\lambda} + \frac{1}{2} - \gamma_E - \psi(1-\lambda) + \mathcal{O}(\epsilon) \right]. \quad (39)$$

According to Eq. (18) we thus get

$$B_{V_C}^{\overline{\text{MS}}} = 2m_r C_F \alpha_s \left(-\frac{1}{2\lambda} - \frac{1}{2} \ln \left(\frac{-8m_r E}{\mu^2} \right) + \frac{1}{2} - \gamma_E - \psi(1-\lambda) \right). \quad (40)$$

Turning to finite- r regularization the Coulomb Green function reads

$$G_c^{(r)}(E) = \frac{m_r^2 C_F \alpha_s}{\pi} \left[\frac{1}{2m_r C_F \alpha_s r_0} - \ln(\mu e^{\gamma_E} r_0) - \frac{1}{2\lambda} - \frac{1}{2} \ln \left(\frac{-8m_r E}{\mu^2} \right) + 1 - \gamma_E - \psi(1-\lambda) \right]. \quad (41)$$

whereas $u_0(r_0)$ for the Coulomb case is given by

$$u_0(r_0) = 1 - 2m_r r_0 C_F \alpha_s \ln(\mu e^{\gamma_E} r_0). \quad (42)$$

The expression stops at $\mathcal{O}(\alpha_s)$. In the Coulomb approximation there are no $\mathcal{O}(\alpha_s^2)$ terms in $u_0(r_0)$ and, therefore, in $A_{V_C}^{(r)}$. Using Eq. (34) we then find

$$B_{V_C}^{(r)}(E) = 2m_r C_F \alpha_s \left[-\frac{1}{2\lambda} - \frac{1}{2} \ln \left(\frac{-8m_r E}{\mu^2} \right) + 1 - \gamma_E - \psi(1-\lambda) \right]. \quad (43)$$

Note that in an strict NNLO or NNLL computation of the decay ratio this would be the only term that should be considered.

Thus we compute $c_r^{\overline{\text{MS}}}$ in an expansion in α_s and obtain³

$$c_r^{\overline{\text{MS}}} = -2m_r \frac{C_F \alpha_s}{2} + \mathcal{O}(\alpha_s^2). \quad (45)$$

This constant can also be obtained from the difference between dimensional- and r -regularized computations at finite order in α_s . At the lowest order it

³If the constant e^{γ_E} were not introduced in Eq. (35), $c_r^{\overline{\text{MS}}}$ would read

$$c_{(r)}^{\overline{\text{MS}}} = -2m_r C_F \alpha_s \left(\frac{1}{2} - \gamma_E \right) + \mathcal{O}(\alpha_s^2). \quad (44)$$

corresponds to the computation of one- and two-loop contributions to the Green function in both schemes, by considering the difference of their renormalized pieces. We have checked in an explicit calculation that Eq. (45) is reproduced by the difference of two-loop contributions.

In order to obtain the $\mathcal{O}(\alpha_s^2)$ corrections to $c_r^{\overline{\text{MS}}}$ one has to include the $\mathcal{O}(\alpha_s^2)$ corrections to the static potential and compute the associated corrections to the Green function in both schemes. In principle, this is possible and partial results can be found in the literature. Nevertheless, this would go beyond the aim of this work, since it would produce corrections that are anyway unmatched by the precision of the hard matching coefficient.

Finally, for a general potential with the right short distance structure, we can combine Eq. (21) with Eqs. (37) and (45) and write

$$\delta\rho_n^{\overline{\text{MS}}}(\mu) = -\frac{8m_r C_F}{3m_1 m_2} D_{S^2,s}^{(2)}(\mu) \left(\hat{B}_{V_s^{(0)}}^{(r)}(E_n^{(0)}; \mu) + \frac{1}{3} m_r C_F \alpha_s + \mathcal{O}(\alpha_s^2) \right). \quad (46)$$

Once we know the $\overline{\text{MS}}$ expression we can also write $\delta\rho_n$ in different schemes. For instance, in the "hard-matching" scheme used in Ref. [12] we have

$$\delta\rho_n^{HM}(\mu) = -\frac{8m_r C_F}{3m_1 m_2} D_{S^2,s}^{(2)}(\mu) \left(\hat{B}_{V_s^{(0)}}^{(r)}(E_n^{(0)}; \mu) - 2m_r C_F \alpha_s + \mathcal{O}(\alpha_s^2) \right), \quad (47)$$

which will be relevant afterwards.

These results enable us to compute the decay ratio in terms of $\hat{B}_{V_s^{(0)}}^{(r)}$, whose determination will be discussed in the next section.

6 Determination of $\hat{B}_{V_s^{(0)}}^{(r)}$

In this section we determine $\hat{B}_{V_s^{(0)}}^{(r)}(E_n^{(0)})$ in several approximation schemes for $V_s^{(0)}$. We have already mentioned that our idea is to treat the static potential exactly, yet we only know its expression up to three loops. There is some freedom on how this truncation is performed. This produces a class of potentials to study, which introduces some scheme and scale uncertainties. As we have stressed in previous sections, the analysis applies to any arbitrary potential with the correct short distance behavior and not unbounded from below at long distances. Therefore, in what follows we will consider different approximations to the static potential. One quality that they have in common is the renormalon cancellation. We have to preserve renormalon cancellation between the static potential and the pole mass of the heavy quark. At the same time we will be forced to consider the resummation of logarithms to reproduce the correct behavior of the

potential at short distances. Thus we will have to devise schemes where both the resummation of the logarithms and the renormalon cancellation is achieved order by order in the perturbative expansion. We illustrate this discussion in the following sections, where we show the determination of $B_{V_s^{(0)}}^{(r)}$ using either the Coulomb potential, the static potential at different orders in $\alpha_s(\mu)$, and the static potential at different orders in $\alpha_s(1/r)$. In this last case we will use different schemes with renormalon cancellation. The dependence on the scheme of renormalon subtraction (potential) may give an estimate of the error, since it is also a measure of the dependence on the long distance behavior of the potential.

Finally, let us note as well that, in order for our computation to make sense, the successive approximations to the static potential should be convergent (or at least small) themselves. We will check this convergence in this section.

6.1 Coulomb potential

If we approximate the static potential by the Coulomb potential V_C we can get an analytic solution for $\hat{B}_{V_C}^{\overline{\text{MS}}}$ by directly working in dimensional regularization. Expanding $G_c^{(D)}(E)$ as given in Eq. (39) around its poles at $E_n^{(0)} \equiv -m_r C_F \alpha_s^2 / (2n^2)$ we can write

$$G_c^{(D)}(E) = -\frac{\alpha_s C_F m_r^2}{\pi} \frac{2 E_n^{(0)}}{n(E_n^{(0)} - E)} + \hat{G}_c^{(D)}(E_n^{(0)}) + \mathcal{O}(E - E_n^{(0)}) \quad (48)$$

with

$$\hat{G}_c^{(D)}(E_n^{(0)}) = \frac{g^2 C_F m_r^2}{4\pi^2} \left(\frac{-8m_r E}{4\pi e^{-\gamma_E}} \right)^{-2\epsilon} \left[\frac{1}{4\epsilon} + \frac{1}{2} - \gamma_E + \frac{1}{n} - \psi(n) + \mathcal{O}(\epsilon) \right]. \quad (49)$$

Comparing to Eq. (19) we obtain

$$\hat{B}_{V_C}^{\overline{\text{MS}}}(E_n^{(0)}) = 2m_r C_F \alpha_s \left(-\frac{1}{2} \ln \frac{-8m_r E_n^{(0)}}{\mu^2} + \frac{1}{2} - \gamma_E + \frac{1}{n} - \psi(n) \right) \quad (50)$$

and thus $\delta\rho_n^{\overline{\text{MS}}}(\mu)$ in the Coulomb approximation directly from Eq. (21).

6.2 Fixed order $V_s^{(0)}$: $\alpha_s(\mu_s)$ expansion

The standard way to go beyond the Coulomb potential approximation for the static potential is to make an expansion in $\alpha_s(\mu_s)$. Thus we write

$$\tilde{V}_{SD}(q) = -\frac{4\pi C_F \alpha_s(\mu_s)}{q^2} \left(1 + \sum_{n=1}^{\infty} \left(\frac{\alpha_s(\mu_s)}{4\pi} \right)^n \tilde{a}_n(\mu_s; q) \right). \quad (51)$$

This expanded version of the static potential is often used in quarkonium phenomenology to respect rigorous expansion according to non-relativistic power counting⁴. In position space we have

$$\lim_{r \rightarrow 0} V_s^{(0)}(r) = V_{SD}(r) = -\frac{C_F \alpha_s(\mu_s)}{r} \left\{ 1 + \sum_{n=1}^{\infty} \left(\frac{\alpha_s(\mu_s)}{4\pi} \right)^n a_n(\mu_s; r) \right\} \quad (52)$$

In practice we will take the static potential up to NNNLO, i.e. up to $\mathcal{O}(\alpha_s^4)$ including also the leading ultrasoft corrections. This means we take into account the first three terms of this expansion with coefficients

$$\begin{aligned} a_1(\mu_s; r) &= a_1 + 2\beta_0 \ln(\mu_s e^{\gamma_E} r) , \\ a_2(\mu_s; r) &= a_2 + \frac{\pi^2}{3} \beta_0^2 + (4a_1\beta_0 + 2\beta_1) \ln(\mu_s e^{\gamma_E} r) + 4\beta_0^2 \ln^2(\mu_s e^{\gamma_E} r) , \\ a_3(\mu_s; r) &= a_3 + a_1\beta_0^2\pi^2 + \frac{5\pi^2}{6} \beta_0\beta_1 + 16\zeta_3\beta_0^3 \\ &\quad + \left(2\pi^2\beta_0^3 + 6a_2\beta_0 + 4a_1\beta_1 + 2\beta_2 + \frac{16}{3}C_A^3\pi^2 \right) \ln(\mu_s e^{\gamma_E} r) \\ &\quad + \left(12a_1\beta_0^2 + 10\beta_0\beta_1 \right) \ln^2(\mu_s e^{\gamma_E} r) + 8\beta_0^3 \ln^3(\mu_s e^{\gamma_E} r) \\ &\quad + \delta a_3^{us}(\mu_s, \mu_{us}), \end{aligned} \quad (53)$$

Explicit expression for $a_i(\mu_s; r)$ can be found in the literature [30, 31, 32, 33, 34, 35, 36]. For the ultrasoft corrections to the static potential we take

$$\delta a_3^{us}(\mu_s, \mu_{us}) \simeq \frac{16}{3} C_A^3 \pi^2 \ln \left(\frac{\mu_{us}}{\mu_s} \right). \quad (54)$$

We will not consider the renormalization group improved ultrasoft contribution in this paper as its numerical impact is small. The potential is shown in Figure 1 (dashed lines) for $\mu_s = 2$ GeV and the number of light flavors set to $N_l = 4$. It is clear that for small r , depicted in the inset of Figure 1, there are serious issues regarding the convergence. The potential changes drastically in going from LO to NLO to NNLO etc. This behavior occurs for the typical values of μ_s and N_l that apply for the charm and bottom case. As one increases the value of μ_s , one has to go to shorter distance to see this effect, as it would happen for top.

Ignoring this problem for the moment and working with the Fixed Order (FO) static potential we can obtain $u_0(r_0)$ and, therefore, $A_{V_s^{(0)}}^{(r)}(r_0)$ as an expansion in α_s as well. We find

$$A_{V_s^{(0)}}^{(r)}(r_0) = \frac{1}{r_0} - 2m_r \alpha_s(\mu) C_F v(l_0),$$

⁴In the most rigorous fixed order computation only the Coulomb part of the static potential is treated exactly and α_s corrections corresponding to the second and remaining terms in Eq.(51) are treated iteratively order by order by insertion.

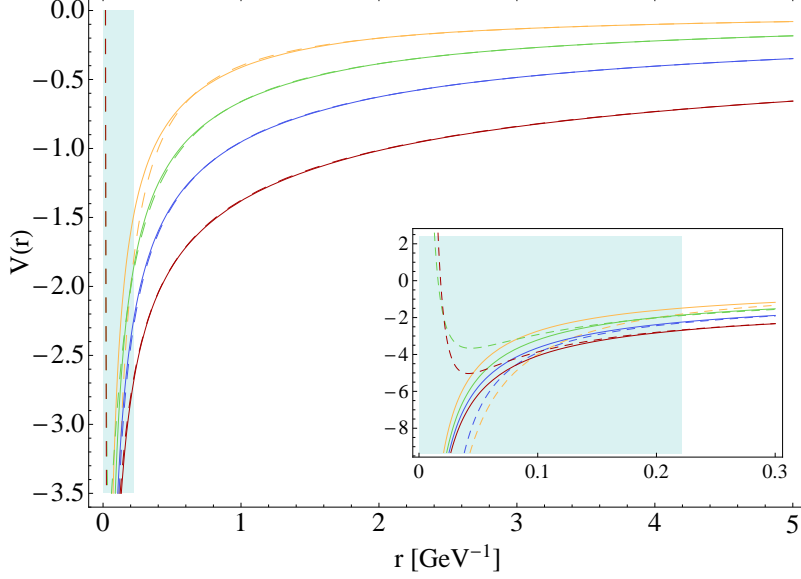


Figure 1: The FO (dashed) and RGI (solid) static potential $V_{SD}(r)$ according to Eq. (52) and Eq. (59) respectively. We take $\mu_s = 2$ GeV, $N_l = 4$ and $\mu_r = 2$ GeV. The potential is shown as a function of r at LO (yellow), NLO (green), NNLO (blue) and NNNLO (red) with the small r region shown in the inset. The shaded area in blue indicates the short distance regime $0 < r < 1/m_b$.

$$v(l_0) = \sum_{i=0}^3 v_n(l_0) \left(\frac{\alpha_s(\mu)}{4\pi} \right)^n, \quad (55)$$

where $l_0 = \ln(\mu e^{\gamma_E} r_0)$ and the expansion coefficients are given by

$$\begin{aligned} v_0(l_0) &= l_0, \\ v_1(l_0) &= (a_1 - 2\beta_0) l_0 + \beta_0 l_0^2, \\ v_2(l_0) &= \left(a_2 - 4a_1\beta_0 + 8\beta_0^2 + \frac{\pi^2}{3}\beta_0^2 - 2\beta_1 \right) l_0 \\ &\quad + \left(2a_1\beta_0 - 4\beta_0^2 + \beta_1 \right) l_0^2 + \frac{4\beta_0^2}{3} l_0^3, \\ v_3(l_0) &= \left(a_3 + \delta a_3^{us} - 6a_2\beta_0 + 24a_1\beta_0^2 + a_1\beta_0^2\pi^2 - (48 + 2\pi^2)\beta_0^3 - 4a_1\beta_1 \right. \\ &\quad \left. + \left(20 + \frac{5\pi^2}{6} \right) \beta_0\beta_1 - 2\beta_2 + 16\beta_0^3\zeta_3 - \frac{16}{3}\pi^2 C_A^3 \right) l_0 \\ &\quad + \left(3a_2\beta_0 - 12a_1\beta_0^2 + (24 + \pi^2)\beta_0^3 + 2a_1\beta_1 - 10\beta_0\beta_1 + \beta_2 + \frac{8\pi^2}{3}C_A^3 \right) l_0^2 \\ &\quad + \left(4a_1\beta_0^2 - 8\beta_0^3 + \frac{10}{3}\beta_0\beta_1 \right) l_0^3 + 2\beta_0^4 l_0^4. \end{aligned} \quad (56)$$

The μ dependence appearing in Eq. (55) enters through Eq. (29) and should be cancelled in Eq. (6). Even though the exact expression for the static potential is scale independent, working at a finite order in $\alpha_s(\mu_s)$ there is some residual μ_s dependence.

The computation of $B_{V_s^{(0)}}^{(r)}$ is done numerically along the lines of Section 5. We use the input values $m_{b,\text{PS}}(2\text{ GeV}) = 4.515\text{ GeV}$ [37] and $m_{c,\text{PS}}(0.7\text{ GeV}) = 1.50\text{ GeV}$ [38] for bottom and charm quarks, respectively. They can be translated into scale-invariant $\overline{\text{MS}}$ -mass of $\overline{m}_b = 4.19\text{ GeV}$ and $\overline{m}_c = 1.25\text{ GeV}$. The strong coupling $\alpha_s^{(n_f=5)}(M_z) = 0.118$ is used as an input evolved down to low energy scale using 4-loop running formulae. For the top quark mass we use $m_{t,\text{PS}}(20\text{ GeV}) = 173\text{ GeV}$ for illustration. The scale μ_{us} needed for the leading ultrasoft contribution is set to $\mu_{us} = 0.7\text{ GeV}$ for charm, $\mu_{us} = 1\text{ GeV}$ for bottom and $\mu_{us} = 10\text{ GeV}$ for top.

In Figure 2 we show the results for charm, bottom and top (dashed lines) as a function of the scale μ_s for fixed μ . For illustration we have chosen $\mu = 1.5\text{ GeV}$ for charm, 2 GeV for bottom and 20 GeV for top. Note that, ideally, the result should be independent of μ_s , as it reflects a dependence on the long distance behavior of the potential. For charm and bottom we see problems of convergence, in particular for small values of μ_s . This is due to the behavior of the potential at short distances, which we have already illustrated in Figure 1. For top the situation is much better. Note that the LO curve corresponds to the Coulomb potential. In all three cases we observe a significant gap between the Coulomb solution and the higher order corrections (for the range of μ_s for which the result can be trusted).

Before we address the problem of the bad convergence, let us remark that expanding the potential in $\alpha_s(\mu)$, the pole mass renormalon enters as an r -independent constant in the potential. This constant cancels in the evaluation of $B_{V_s^{(0)}}^{(r)}$, which is independent of the overall normalization of the potential. Thus, in this evaluation the dependence will only enter in the values of the mass used. The error associated to this uncertainty is beyond our accuracy.

6.3 RG-Improved $V_s^{(0)}$: $\alpha_s(1/r)$ expansion

In the previous subsection we have seen that the convergence for $\widehat{B}_{V_s^{(0)}}^{(r)}$ is very unsatisfactory if we use Eq. (52). Surprisingly the problem comes from short and not long distances. The solution is to absorb the large logarithms into the running coupling. However, this has to be done carefully in order not to destroy the renormalon cancellation achieved order by order in α_s . More specifically, we

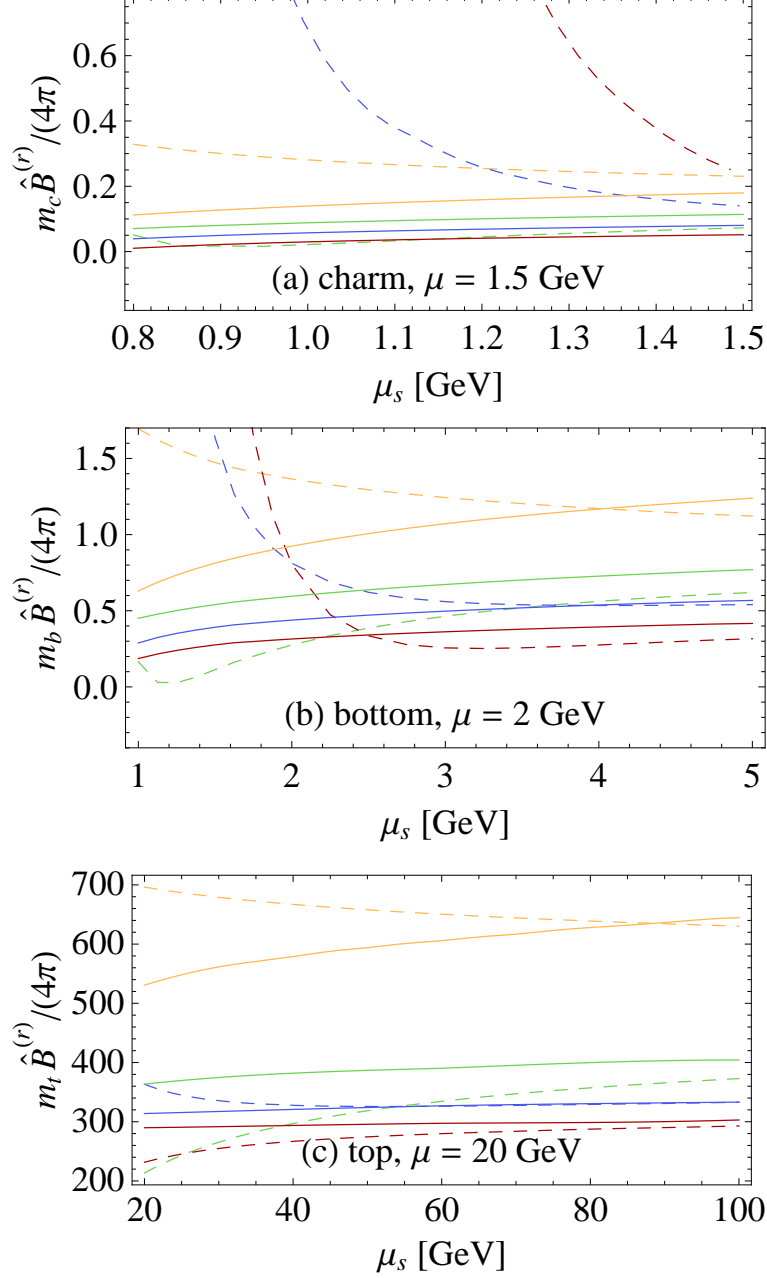


Figure 2: $\hat{B}_{V_s^{(0)}}^{(r)}$ as a function of μ_s at LO(yellow), NLO(green), NNLO(blue) and NNNLO(red) with $\mu = 1.5$ GeV for charm, 2 GeV for bottom, and 20 GeV for top. Dashed lines are obtained using Eq. (52), solid lines are obtained using Eq. (59).

consider different approximations to the static potential behaving for $r \rightarrow 0$ as

$$V_s^{(0)} \simeq -\frac{C_F \alpha_s(1/r)}{r} \left\{ 1 + \sum_{n=1}^3 a_n(1/r; r) \left(\frac{\alpha_s(1/r)}{4\pi} \right)^n \right\}, \quad (57)$$

and yet achieving renormalon cancellation order by order in $\alpha_s^n(1/r)$. This will give us an estimate of the dependence of the result on the long distance behavior of the potential. We will generically name this class of potentials renormalization group improved (RGI) and denote them by LO, NLO, ... according to the power of $\alpha_s(1/r)$ at which we stop the perturbative expansion in Eq. (57).

One possibility that fulfills all these requirements is the PS scheme [39] with the following modification:

$$V_{PS}(r) = V_{SD}(r, \mu_r) + 2 \delta m_{PS} \quad (58)$$

with

$$V_{SD}(r, \mu_r) \equiv \int_{q \leq \mu_r} \frac{d^3 \mathbf{q}}{(2\pi)^3} e^{i\mathbf{q} \cdot \mathbf{r}} \tilde{V}_{SD}|_{\mu=\mu_s}(q) + \int_{q > \mu_r} \frac{d^3 \mathbf{q}}{(2\pi)^3} e^{i\mathbf{q} \cdot \mathbf{r}} \tilde{V}_{SD}|_{\mu=q}(q) \quad (59)$$

Thus we introduce a factorization scale μ_r . For $q < \mu_r$ we expand $\tilde{V}_{SD}(q)$ in $\alpha_s(\mu_s)$, as in the previous subsection. For $q > \mu_r$ however, we use the running coupling in $\tilde{V}_{SD}(q)$. As can be seen in Figure 1, the RGI potential (solid lines) shows good convergence for all values of r . We have checked that the results for $\hat{B}_{V_s^{(0)}}^{(r)}$ are not sensitive to the precise value of the factorization scale, as long as μ_r is large enough. This definition has the advantage that the renormalon contribution is r independent and achieves the resummation of logarithms. The fact that the renormalon cancellation is r independent makes it possible to work also with $\delta m_{PS} = 0$ in Eq. (58), as far as the determination of $\hat{B}_{V_s^{(0)}}^{(r)}(E_n^{(0)})$ is concerned.

The results for $\hat{B}_{V_s^{(0)}}^{(r)}$, using Eq. (59) rather than Eq. (52) are depicted as solid lines in Figure 2. We have taken $\mu_r = 1$ GeV, $\mu = 1.5$ GeV for charm, $\mu_r = \mu = 2$ GeV for bottom, and $\mu_r = \mu = 20$ GeV for top. As can be seen, the resummation of logarithms results in a dramatic improvement in the charm and bottom case, and is also quite significant in the top case. In all three cases, the RG result is nearly independent of μ_s . This signals a weak dependence on the long distance tail of the potential. This is to be contrasted with the results obtained using Eq. (52), which are completely unreliable unless unnaturally large values for μ_s are used (especially for charm). The RGI curves show a good convergent pattern for top, and also a reasonable convergence in the case of bottom. Even for charm we see signs of convergence, albeit marginal. In particular, in this case, and to a lesser extent in the case of bottom, the splitting between the NNLO and NNNLO curves is not much smaller than the splitting between the NLO

and NNLO curves. Note, though, that at NNNLO the potential starts to be sensitive to ultrasoft physics, which we do not include in our analysis. In this respect the NNNLO curves are to be considered incomplete (though the explicit dependence on the ultrasoft factorization scale is small). Moreover, at some point the asymptotic behavior of the perturbative series should set in and it cannot be ruled out that we are approaching this regime. Still, we would like to point out the smallness of this splitting compared to the total magnitude of the correction achieved by the reorganization of the perturbative series, which can be estimated by comparing the Coulomb line versus the NNNLO curve. In this respect, even if we consider the splitting between the NNLO and NNNLO curves as an error, its magnitude is rather small compared with the total gap. From this analysis, we conclude that we should use the RGI potential instead of the FO one and we will take this attitude in the rest of the paper.

Another possibility that we explore is the use of the RS or RS' potential [40]. To avoid numerical instabilities, due to the behavior of the potential at long distances, we also modify the potential in the following way:

$$V_{\text{RS}}(r) = \begin{cases} (V_{SD} + 2\delta m_{\text{RS}})|_{\mu=\mu_s} = \sum_{n=0}^{\infty} V_{RS,n} \alpha_s^{n+1}(\mu_s) & \text{if } r > \mu_r \\ (V_{SD} + 2\delta m_{\text{RS}})|_{\mu=1/r} = \sum_{n=0}^{\infty} V_{RS,n} \alpha_s^{n+1}(1/r) & \text{if } r < \mu_r \end{cases} \quad (60)$$

Irrespectively of the potential we use, the short distance behavior of the potential and, consequently, $A^{(r)}(r_0; \mu)$ is the same. The full expression for $A^{(r)}(r_0; \mu)$ is more complicated in these cases than in Section 6.2 and we refrain from giving the general explicit expression and only show (for illustration) how it would look like at the lowest order. If for instance we consider LL running at short distance, namely

$$V_s^{(0)}(r) \simeq -\frac{C_F}{r} \frac{\alpha_s(\mu)}{1 - \frac{\beta_0 \alpha_s}{2\pi} \ln(\mu r)}, \quad (61)$$

we have

$$A^{(r)}(r_0) = \frac{1}{r_0} - 2m_r C_F \alpha_s(\mu) v(l_0). \quad (62)$$

$$v(l_0) = \frac{2\pi}{\beta_0 \alpha_s(\mu)} \left\{ f\left[\gamma_E + \frac{2\pi}{\beta_0 \alpha_s(\mu)} - l_0\right] - f\left[\gamma_E + \frac{2\pi}{\beta_0 \alpha_s(\mu)}\right] \right\}, \quad (63)$$

with $f[x] \equiv e^x \text{Ei}(-x) - \ln x$. The coefficients v_n have an expansion in α_s and l_0

$$\begin{aligned} v(l_0) &= l_0 + \left(\frac{\beta_0 \alpha_s}{4\pi}\right) \left\{ -2(\gamma_E + 1)l_0 + l_0^2 \right\} \\ &+ \left(\frac{\beta_0 \alpha_s}{4\pi}\right)^2 \left\{ (8 + 8\gamma_E + 4\gamma_E^2) l_0 - (4 + 4\gamma_E)l_0^2 + \frac{4}{3}l_0^3 \right\} + \dots \end{aligned} \quad (64)$$

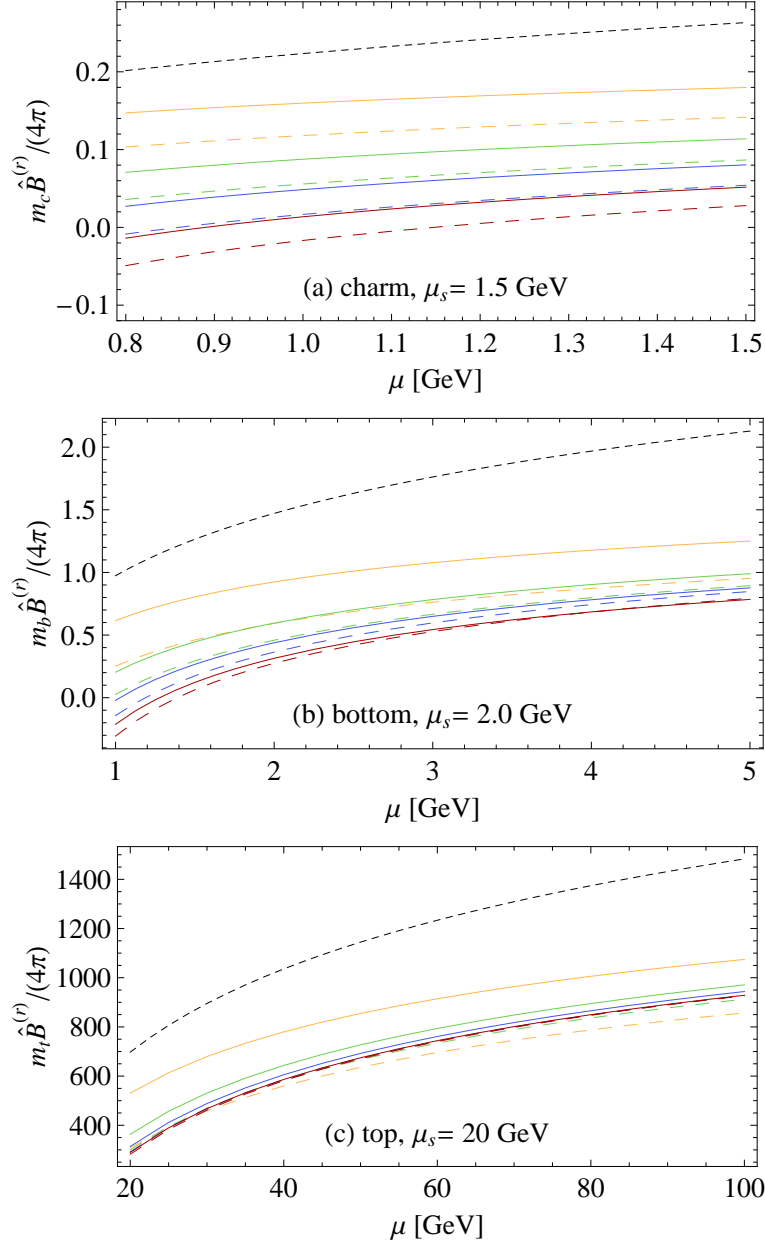


Figure 3: $\hat{B}_{V_s(0)}^{(r)}$ as a function of μ at LO (yellow), NLO (green), NNLO (blue) and NNNLO (red) with $\mu_s = 1.5$ GeV, $\mu_r = 1$ GeV and $\mu_F = \mu_{us} = 0.7$ GeV for charm, $\mu_s = \mu_r = \mu_F = 2$ GeV and $\mu_{us} = 1$ GeV for bottom, and $\mu_s = \mu_r = \mu_F = 20$ GeV, and $\mu_{us} = 10$ GeV for top. Solid lines are obtained in the PS scheme using Eq. (59) and dashed lines are obtained in the RS' scheme using Eq. (60). For reference we also include $\hat{B}_{V_C}^{(r)}$ (short-dashed black line).

We now perform the numerical evaluation of $\widehat{B}_{V_s^{(0)}}^{(r)}$ at different orders in the static potential and compare the results obtained using the PS and RS' scheme. The results are shown in Figure 3. The difference between the schemes is small and converging for the case of bottom and top. In these two cases the differences between both schemes is pretty small for the NNNLO curves. This is again a good signal, since the dependence on the scheme is an indirect measure of the dependence on the long distance tail of the potential. For charm, the situation is less convincing. The gaps between schemes show marginal convergence at best as we increase the order. Yet, this gap is still much smaller than the gap between the Coulomb result and the NNNLO result. Comparing the Coulomb result, shown as the black short-dashed line, to our results, we can see that in all three cases a rather significant portion of the correction is already achieved with the LO RGI potential. In the case of top the NLO RGI potential is already quite close the most accurate NNNLO result. This behavior is also seen, to a lesser extent in the case of bottom. Note that the LO RGI potential exactly incorporates the r -dependent leading logarithms. This is equivalent to introducing an infinite number of corrections to the Coulomb potential and to iterate them an infinite numbers of times. This reorganization of perturbation theory seems to produce a major effect. Another observation is that the RS' scheme produces an accelerated convergence to the asymptotic regime. This is clearly seen in the top case, and to a lesser extent, in the bottom case. In those cases the LO RGI potential produces the bulk of the correction and the magnitude of the higher order corrections is smaller in the RS' than in the PS scheme. The price paid is that the splitting between different orders in the RS' scheme is less convergent.

The dependence of the results on μ_r is very small. Changing μ_r from 2 GeV to 4 GeV for example results in differences that are an order of magnitude smaller than the changes we find by going from say LO to NLO.

The dependence on μ will have to be cancelled by the scale dependence of the matching coefficient $c_s(\mu)$. Note that our evaluation of $\widehat{B}_{V_s^{(0)}}^{(r)}$ also includes subleading logarithms, which are not matched by the precision of the RG (hard) computation. The fact that the scale dependence roughly corresponds to the Coulomb potential (with RG running) can be taken as an indication that sub-leading logarithms are not very important (see Figure 3 for illustration).

Finally, there is also a dependence on the scale μ_s . This dependence (as the dependence on the renormalon subtraction scheme) partly reflects the dependence of the result on the long distance tail of the potential. On the other hand one can not take μ_s very small otherwise $\alpha_s(\mu_s)$ becomes very large. We now perform the numerical evaluation of $\widehat{B}_{V_s^{(0)}}^{(r)}$ at different orders in the loop expansion in the PS scheme and using different values of μ_s . The results for varying values of μ_s are shown as bands in Figure 4. We also show the Coulomb result as the band enclosed by black dashed lines. This plot also illustrates that the bulk of

the correction is already achieved with the LO/NLO RGI potential in the top and bottom case, where we have convergence (in the charm case convergence is marginal at best). The μ_s dependence tends to diminish as one increases the order of the RGI potential in the top, and to a lesser extent in the bottom case. In the charm case the μ_s dependence remains almost constant. Overall, we find that the μ_s dependence is slightly larger than the scheme dependence, but still smaller than the typical gap due to working at different orders in the RGI potential.

7 Phenomenology of the decay ratio

Using the results obtained for $\hat{B}_{V_s^{(0)}}^{(r)}(E_n^{(0)}; \mu)$ we can get improved determinations of the decay ratio, by combining Eqs. (6), (12) and (46) with the determination of c_s from Ref. [12]. We use the results obtained in Section 6.3 with the RGI potential, since they both achieve the resummation of logarithms and renormalon cancellation. The main source of uncertainties in the evaluation of $\hat{B}_{V_s^{(0)}}^{(r)}(E_n^{(0)}; \mu)$ is reflected by the computations at different orders in α_s in the static potential and, to a lesser extent, by the dependence on μ_s . In comparison, the dependence on the quark mass, μ_r , μ_f and μ_{us} is small. Therefore, we will fix those parameters to the values used in Section 6.3. In Section 6.3 we also saw that the scheme dependence for renormalon subtraction was small, compared with the uncertainty due to the computation at different orders. Therefore, we will only take one scheme (PS) for reference in the plots.

In order to explore different power counting expansions for our results, we will consider and compare different approximations. In particular we will show the effect of resumming logarithms in the matching coefficients $D_{S^2, s}^{(2)}$ and c_s . We will see that the RGI in the matching coefficients plays an important role to make the result more factorization scale independent. The results obtained within a strict perturbative expansion (see Ref. [12]) are labelled as LO, NLO and NNLO respectively and, after resummation of logarithms, as LL, NLL and NNLL. Taking into account the static potential exactly, using numerical methods as described in the previous sections, we obtain improved predictions for the relativistic corrections that we label by including "I" to the previous labelling: NLLI (including c_s with NLL precision and the improved relativistic correction $\delta\rho_n$) and NNLLI (c_s with NNLL precision and the improved relativistic correction $\delta\rho_n$). For comparison we will also consider the result without resummation of the logarithms in the matching coefficient, NNLOI (c_s with NNLO precision and the improved relativistic correction $\delta\rho_n$). For both, NNLLI and NNLOI we will consider the results taking the RGI static potential at LO, NLO, NNLO and NNNLO.

From the point of view of a double counting in α_s and v the NLL result (with

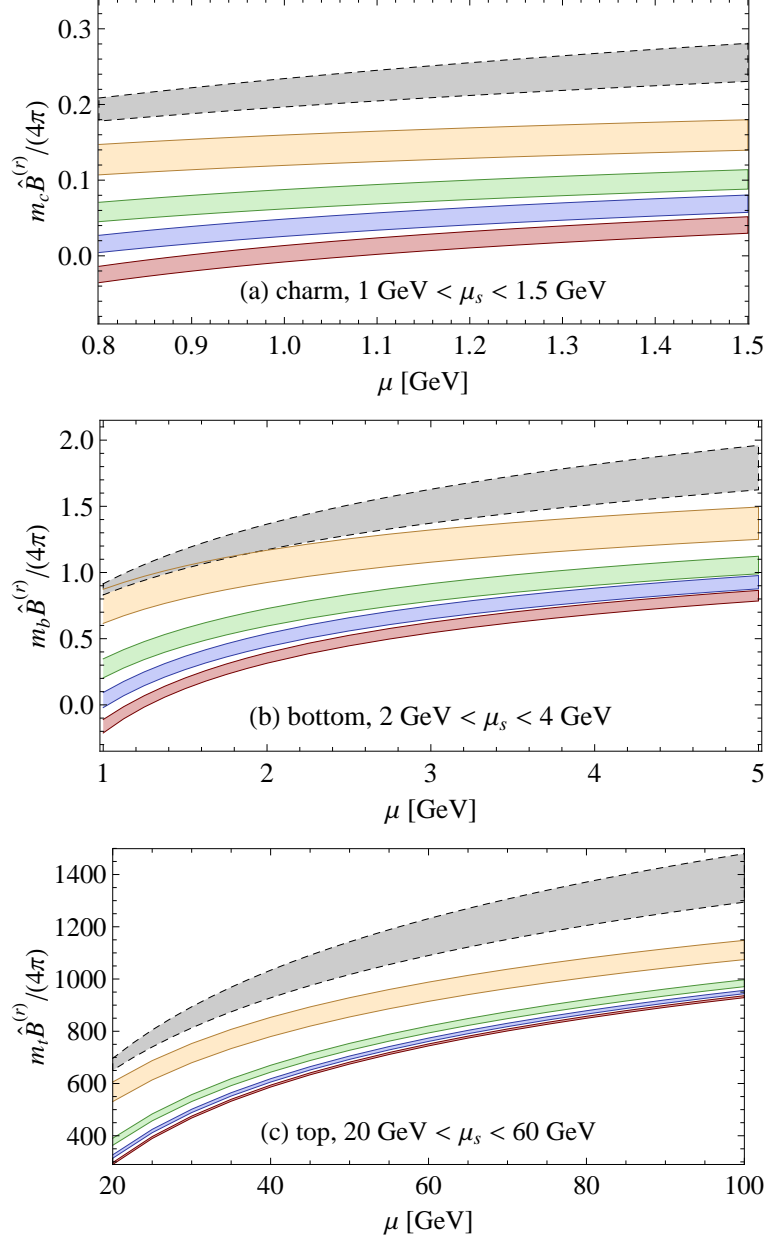


Figure 4: $\hat{B}_{V_s^{(0)}}^{(r)}$ using Eq. (59) as a function of μ at LO (yellow), NLO (green), NNLO (blue) and NNNLO (red) with $\mu_r = 1 \text{ GeV}$ and $\mu_F = \mu_{us} = 0.7 \text{ GeV}$ for charm, $\mu_r = \mu_F = 2 \text{ GeV}$ and $\mu_{us} = 1 \text{ GeV}$ for bottom, and $\mu_r = \mu_F = 20 \text{ GeV}$, and $\mu_{us} = 10 \text{ GeV}$ for top. The bands are obtained by variation of μ_s in the range 1–1.5 GeV, 2–4 GeV and 20–60 GeV for charm, bottom and top respectively. For reference we also include $\hat{B}_{V_C}^{(r)}$ (grey band).

NLL precision for c_s) can be considered as $\mathcal{O}(\alpha_s, v^0)$ whereas NLLI is $\mathcal{O}(\alpha_s, v^2)$ and NNLLI is $\mathcal{O}(\alpha_s^2, v^2)$. As a general trend, moving from NLL to NLLI improves the scale dependence. This is due to the fact that, by using the RGI, NNLO $\mathcal{O}(\alpha_s^2)$ logarithms count as NLL and can be matched with a part of the scale dependence of the relativistic $\mathcal{O}(v^2)$ correction. Note as well that the inclusion of c_s with NNLL precision accounts for $\mathcal{O}(\alpha_s^3)$ leading logarithms and beyond. Those should be cancelled by the inclusion of the subleading scale dependence of the relativistic correction. Most of it is actually built in by the numerical evaluation of the relativistic correction with the RG potential. In principle, this should be reflected in an improvement in the scale dependence in going from NLLI to NNLLI. On the other hand, this double counting in α_s and v scheme produces an unmatched scheme dependence, which can only be matched by working at the same order in α_s and v .

We have also studied the dependence on the specific r -renormalization scheme of $\hat{B}_{V_s^{(0)}}^{(r)}(E_n^{(0)}; \mu)$. This dependence should vanish when combined with $c_r^{\overline{\text{MS}}}$. In particular we have studied the effect of eliminating γ_E in the logarithms in Eq. (35) and consequently using Eq. (44) for $c_r^{\overline{\text{MS}}}$. Note that this is actually equivalent to using $\hat{B}_{V_s^{(0)}}^{(r)}(E_n^{(0)}; \mu e^{-\gamma_E})$. We have checked that (at least in the cases where the series converges) this dependence fades away when considering the potential with increasing accuracy. The reason is that the γ_E terms that appear at higher orders get more accurately described as we increase the order of our computation. This increases our confidence in the perturbative approach. The introduction of γ_E in the scale μ makes the different terms in the expansion approach the asymptotic result faster, but the effect is not very significant.

In the following subsections we will consider in turn the cases of top, bottom and charm.

7.1 Top

We start with the top since it is the cleanest possible case, where we expect best convergence. The scales are fixed as $\mu_F = \mu_r = \mu_s = 20$ GeV and $\mu_{us} = 10$ GeV and we work in the PS scheme.

In Figure 5 we show the decay ratio at NNLOI (dashed lines) and NNLLI (solid lines) at different orders in α_s in the static potential (LO: yellow; NLO: green; NNLO: blue; NNNLO: red). For reference we also include the LL, NLL, and NNLL results (short-dashed lines) obtained within a strict perturbative expansion. Comparing the NNLOI with the NNLLI curves, it can be seen that the inclusion of the RG matching coefficients has a significant impact in reducing the scale dependence. Also, there is a sizable gap when moving from NNLL to NNLLI even if we take the LO RGI static potential (which includes the r run-

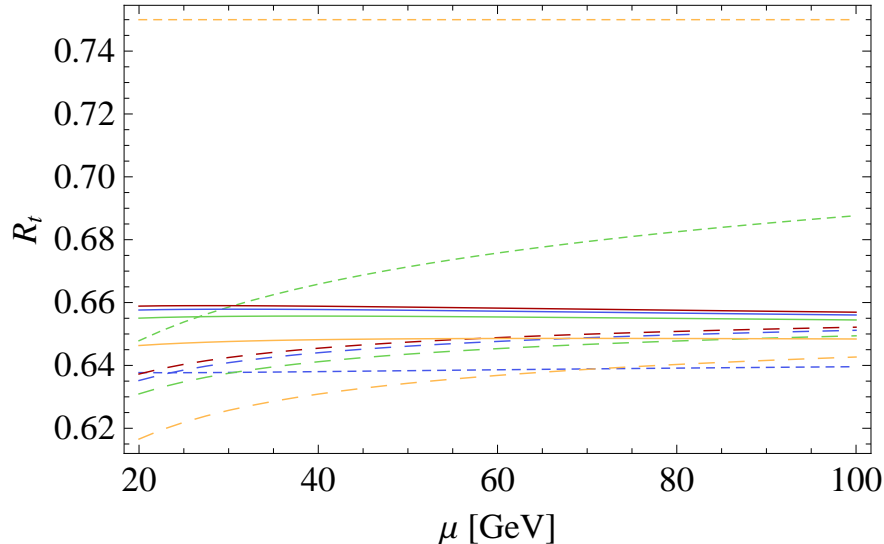


Figure 5: Decay ratio in the PS scheme at NNLOI (dashed) and NNLLI (solid) at different orders in α_s in the static potential ($\mathcal{O}(\alpha_s)$: yellow; $\mathcal{O}(\alpha_s^2)$: green; $\mathcal{O}(\alpha_s^3)$: blue; $\mathcal{O}(\alpha_s^4)$: red). For reference we also include the LL, NLL, and NNLL results (short-dashed).

ning producing the shift we observe in the plot). The inclusion of subleading corrections to the potential produces a convergent effect. Actually, the NLO RGI static potential result is already quite close to the asymptotic result. This may allow to define a counting in v , by taking the asymptotic limit of the series. The potential problem is that this counting in v is scheme dependent.

To study this scheme dependence, in Figure 6 we show the decay ratio at NLLI in the $\overline{\text{MS}}$ and hard-matching scheme (see Ref. [12] and Eq. (47)) and at NNLLI, all of them at $\mathcal{O}(\alpha_s^4)$ in the static potential. These results are compared to the LL, NNL and NNLL results. Moving from NLL to NLLI improves the scale dependence no matter what scheme is used. As we have already discussed, this is due to the fact that, by using the RG, NNLO $\mathcal{O}(\alpha_s^2)$ logarithms count as NLL and can be matched with a part of the scale dependence of the relativistic $\mathcal{O}(v^2)$ correction. On the other hand there is a sizable gap between the NLLI result obtained in the $\overline{\text{MS}}$ and hard-matching scheme. The latter is much closer to the full NNLLI result. The reason is that the two-loop hard correction is much smaller in the hard-matching scheme compared with the $\overline{\text{MS}}$ scheme. This could indicate that the hard-matching scheme leads to a more convergent series but it cannot be ruled out that this smallness is accidental for $\mathcal{O}(\alpha_s^2)$. Therefore, we believe this gap gives a conservative estimate of the remaining uncertainties. Note that it is much larger than the other sources of uncertainties considered in this paper. For instance, we have also investigated the μ_s dependence and observed that it gets smaller when we consider higher orders in the static potential, pointing to

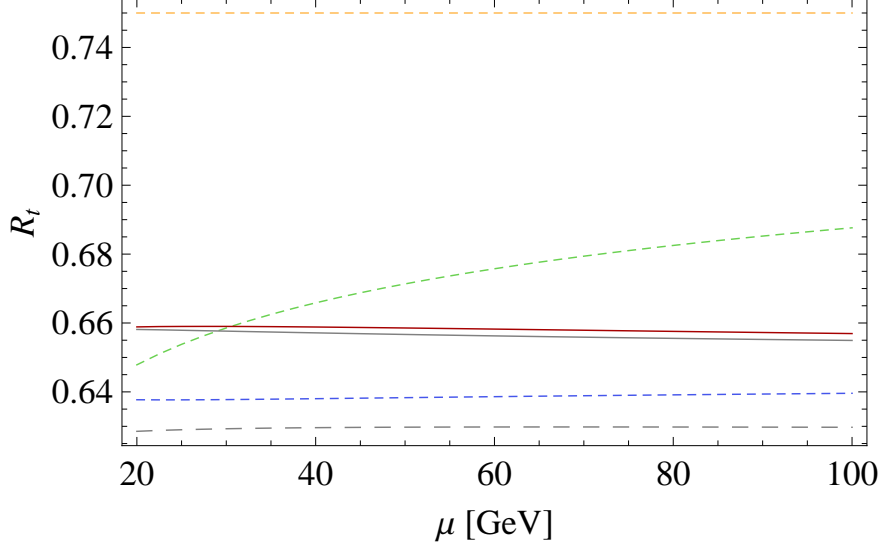


Figure 6: Decay ratio in the PS scheme at NLLI in the $\overline{\text{MS}}$ (grey dashed) and hard-matching scheme (grey solid) and at NNLLI (red solid). For reference we also include the LL, NLL, and NNLL results.

the fact that the long-distance tail of the potential does not have a significant impact on the determination of the decay ratio. A similar comment applies to the renormalon scheme dependence. Therefore, in summary we find nice convergence in the top quark case.

7.2 Bottom

Turning to the bottom case, in Figure 7 we show the decay ratio in the PS scheme at NNLOI and NNLLI at different orders in α_s in the static potential. For reference we also include the LL, NLL, and NNLL results. We use $\mu_r = \mu_F = \mu_s = 2$ GeV and $\mu_{us} = 1$ GeV. Again we can see that the inclusion of the RG matching coefficients has a significant impact in reducing the scale dependence. As in the top case, there is a sizable gap when moving from NNLL to NNLLI. The bulk of it is already obtained by taken the NLO(LO) RGI static potential in the PS(RS') scheme. The inclusion of subleading corrections to the potential produces a smaller effect, yet sizable. Compared to the top case the magnitude of the corrections is larger and the convergence using the static potential at different orders is worse, in particular in going from the $\mathcal{O}(\alpha_s^3)$ to the $\mathcal{O}(\alpha_s^4)$ approximation of the static potential. Nevertheless, one can still see a band (though much wider than for top) where to roughly define a counting in v . We should also stress that using the $\mathcal{O}(\alpha_s^4)$ RGI potential has some ambiguities, since ultrasoft effects enter at this order. Therefore, it can not be considered complete.

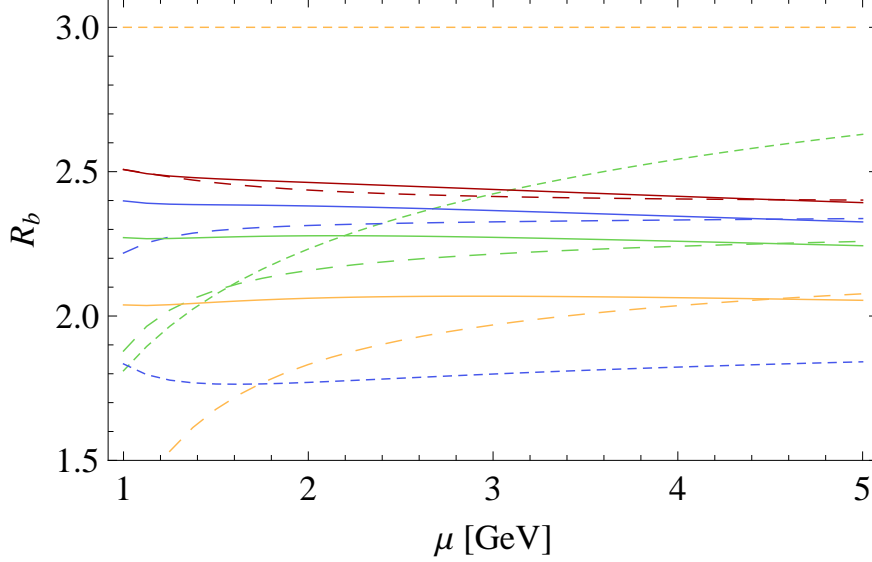


Figure 7: Decay ratio in the PS scheme at NNLOI (dashed) and NNLI (solid) at different orders in α_s in the static potential ($\mathcal{O}(\alpha_s)$: yellow; $\mathcal{O}(\alpha_s^2)$: green; $\mathcal{O}(\alpha_s^3)$: blue; $\mathcal{O}(\alpha_s^4)$: red). For reference we also include the LL, NLL, and NNLL results (short-dashed).

We study the scheme dependence in Figure 8, showing the decay ratio at NLLI in the $\overline{\text{MS}}$ and hard-matching scheme and at NNLI. In all cases the static potential is taken at $\mathcal{O}(\alpha_s^4)$. These results are compared with the LL, NLL and NNLL results. The general pattern of the results is similar to the top case. Moving from NLL to NLLI improves the scale dependence irrespective of the scheme used. However, there is a sizable gap between the NLLI result obtained in the $\overline{\text{MS}}$ and hard-matching scheme, the latter is much closer to the full NNLI result. As for top, we take this gap for a conservative estimate of the remaining uncertainty. Again, this gap is larger than other sources of uncertainties considered in this paper, like the splitting associated to different orders in the static potential, the μ_s or renormalon scheme dependence. Either way the errors are obviously larger here than in the top case. In particular we have found a larger sensitivity to μ_s and the specific implementation of the initial conditions.

We use this analysis to obtain an updated prediction for $\Gamma(\eta_b(1S) \rightarrow \gamma\gamma)$. For the central value we use the NNLI result with $\mu = 2$ GeV and the set of parameters described before, obtaining 0.544 keV. The theoretical error has been estimated considering the difference between the NLLI (in the $\overline{\text{MS}}$) and NNLI result for $\mu = 2$ GeV. We obtain 0.146 keV for this error. As we have already mentioned, we have checked that the uncertainties due the variation of these parameters, the scheme, or the consideration of different order in α_s in

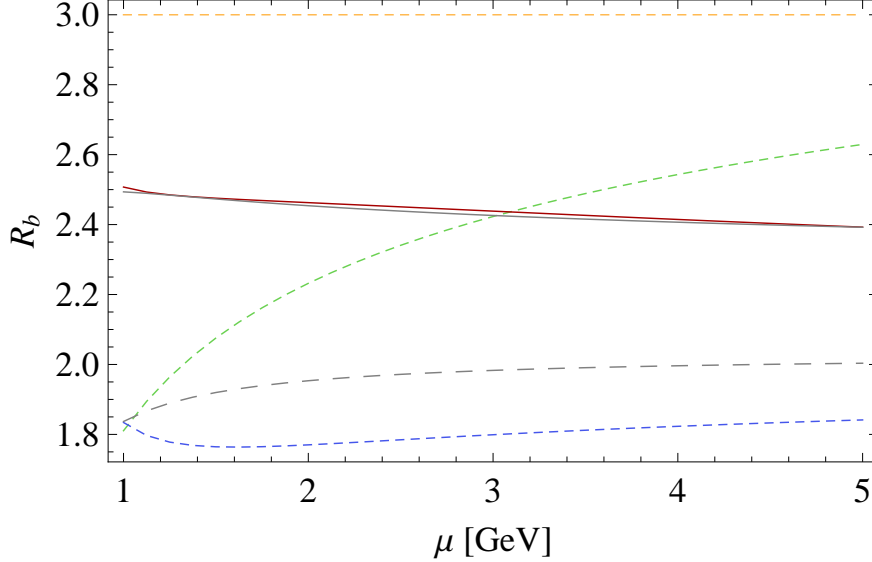


Figure 8: Decay ratio in the PS scheme at NLLI in the $\overline{\text{MS}}$ (grey dashed) and hard-matching scheme (grey solid) and at NNLLI (red solid). For reference we also include the LL, NLL, and NNLL results.

the potential, is much smaller than the error quoted. Another source of error is experimental, coming from $\Gamma(\Upsilon(1S) \rightarrow e^+e^-) = 1.340 \pm 0.018$ keV [41]. This produces a very small error: ± 0.007 keV. Finally, we have also computed the error associated to the indetermination of $\alpha_s(M_z) = 0.118 \pm 0.003$. This error is even smaller: $^{+0.002}_{-0.004}$ keV. We combine the last two errors in quadrature and add linearly to the theoretical error (which completely dominates the error). After rounding we obtain $\Gamma(\eta_b(1S) \rightarrow \gamma\gamma) = 0.54 \pm 0.15$ keV.

7.3 Charm

Finally we consider the charmonium ground state. The applicability of our weak coupling approach to this system is doubtful. Nevertheless, we will find it rewarding that the reorganization of the perturbative expansion significantly improves the agreement with the experimental data. Again we will use the PS scheme and set $\mu_s = 1.5$ GeV, $\mu_r = 1$ GeV and $\mu_F = 1 = \mu_{us} = 0.7$ GeV.

In Figure 9 we show the decay ratio at NNLOI and NNLLI at different orders in α_s in the static potential. For reference we also include the LL, NLL, and NNLL results. The experimental result, using $\Gamma(J/\psi \rightarrow e^+e^-) = 5.55 \pm 0.14$ keV and $\Gamma(\eta_c \rightarrow \gamma\gamma) = 7.2 \pm 0.7 \pm 2.0$ keV [41] is shown as the light blue band, with the central value indicated by the horizontal solid light blue line. Once more we can see that the inclusion of the RG matching coefficients improves the scale

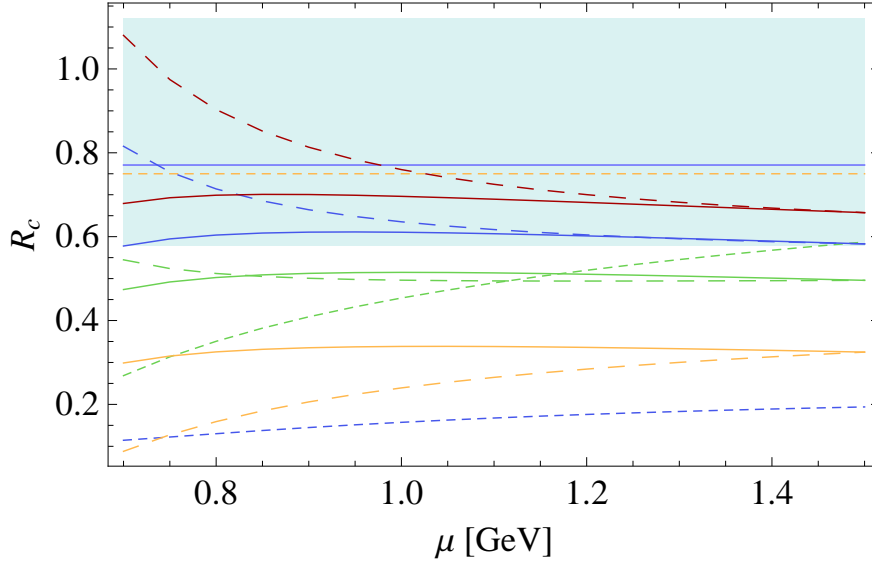


Figure 9: Decay ratio in the PS scheme at NNLOI (dashed) and NNLLI (solid) at different orders in α_s in the static potential ($\mathcal{O}(\alpha_s)$: yellow; $\mathcal{O}(\alpha_s^2)$: green; $\mathcal{O}(\alpha_s^3)$: blue; $\mathcal{O}(\alpha_s^4)$: red). For reference we also include the LL, NLL, and NNLL results (short-dashed). The light blue band represents the experimental error of the ratio where the central value is given by the horizontal solid line.

dependence and there is a sizable gap when moving from NNLL to NNLLI. The inclusion of subleading corrections to the potential produces a slightly smaller though still quite large effect. Compared to the bottom case the magnitude of the corrections is larger and the convergence is worse. We find the same problem in the associated evaluations of the energy and the wave function at the origin. Despite these shortcomings, the effect goes in the direction of bringing agreement with experiment.

We study the scheme dependence by showing the decay ratio at NLLI in the $\overline{\text{MS}}$ and hard-matching scheme and at NNLLI in Figure 10. The static potential is taken at $\mathcal{O}(\alpha_s^4)$. The discussion is pretty similar to the top and bottom case. Moving from NLL to NLLI improves the scale dependence no matter what scheme is used. On the other hand there is a sizable gap between the NLLI result obtained in the $\overline{\text{MS}}$ and hard-matching scheme, the latter being much closer to the full NNLLI result. The reason is the same as for top and bottom. Taking this gap for an estimate of the typical size of the uncertainties produces an error of around 50% in the ratio. This encodes most of the experimental band and it is significantly larger than the typical split produced by working at different orders in α_s in the static potential.

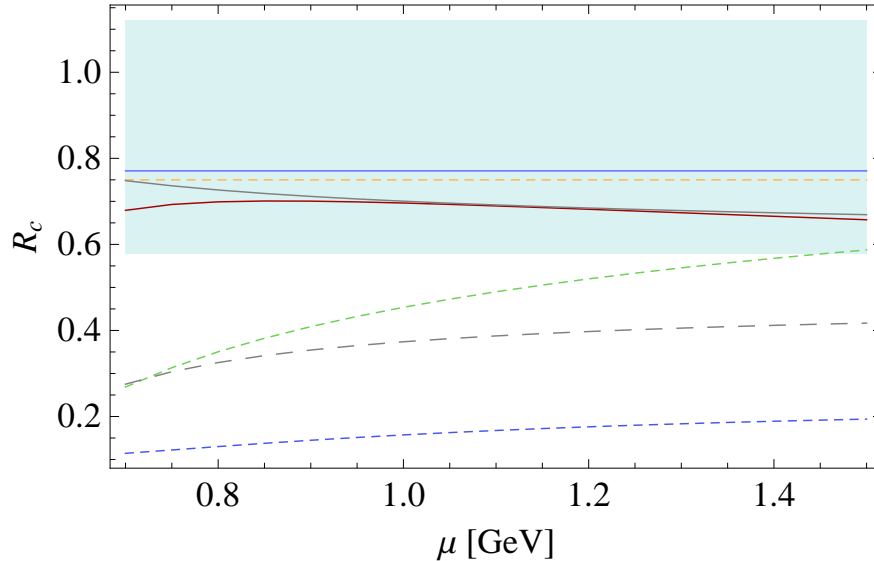


Figure 10: Decay ratio in the PS scheme at NLLI in the $\overline{\text{MS}}$ (grey dashed) and hard-matching scheme (grey solid) and at NNLLI (red solid). For reference we also include the LL, NLL, and NNLL results and the experimental ratio.

8 Conclusions

We have considered a different power counting in potential NRQCD by incorporating the static potential exactly in the leading order Hamiltonian. In this scheme we compute the leading relativistic corrections to the inclusive electromagnetic decay ratios. The effect of this new power counting is dramatic for charm, large for bottom, and sizable even for top. In the case of bottom, we produce an updated value for the η_b decay to two photons

$$\Gamma(\eta_b(1S) \rightarrow \gamma\gamma) = 0.54 \pm 0.15 \text{ keV}. \quad (65)$$

In the case of charmonium, this scheme brings consistency between the weak coupling computation and the experimental value of the decay ratio, but the theoretical error is large.

It is worth emphasizing that in the case where our expansion is more reliable, i.e. the top and bottom case, the bulk of the correction comes from using the first two orders of the RGI potential. The effect of higher-order corrections in the RGI potential is relatively small. The details of the importance of higher-order corrections depends on the scheme. In the RS' already the LO RGI potential gives the bulk of the correction whereas in the PS two terms in the expansion are needed. Irrespectively, they both converge as one goes to higher orders.

This approach could open the possibility to reorganize the perturbative series

in a controlled way. We stress again that this is also relevant for top. Therefore, it is not a strong coupling effect but rather reflects the need of a more optimal resummation of perturbation theory. This might call for a reanalysis of previous results in this new scheme. It is an open question whether there is a similar effect in the case of the hyperfine splitting. We leave this discussion for a forthcoming paper.

It would be misleading to only assign a theoretical error from the scale dependence. This is particularly obvious in the charm case, where the scale dependence by no means reflects a reasonable estimate of the size of higher-order corrections, which are difficult to estimate and can only be inferred from the apparent convergence of the expansion.

Our formalism is flexible enough so that, with little effort, we could replace the perturbative static potential by any potential, in particular, by one fitted to non-perturbative lattice data. This could be of particular relevance for charmonium but it could also be of help for bottomonium, provided the static potential is known with enough accuracy in the unquenched approximation. This would eliminate the error associated to higher order terms in the static potential, but not the error due to higher order terms in the hard matching coefficient and the associated RG improvement.

References

- [1] W. E. Caswell and G. P. Lepage, Phys. Lett. B **167**, 437 (1986).
- [2] A. Pineda and J. Soto, Nucl. Phys. Proc. Suppl. **64** (1998) 428 [arXiv:hep-ph/9707481].
- [3] N. Brambilla, A. Pineda, J. Soto and A. Vairo, Rev. Mod. Phys. **77**, 1423 (2005).
- [4] A. Pineda, PoSEFT09, 017 (2009).
- [5] B. A. Kniehl, A. A. Penin, A. Pineda, V. A. Smirnov and M. Steinhauser, Phys. Rev. Lett. **92**, 242001 (2004).
- [6] B. Aubert *et al.* [BABAR Collaboration], Phys. Rev. Lett. **101**, 071801 (2008) [E-ibid. **102**, 029901 (2009)].
- [7] G. Bonvicini *et al.* [The CLEO Collaboration], arXiv:0909.5474 [hep-ex].
- [8] A. Pineda and A. Signer, Nucl. Phys. B **762**, 67 (2007).
- [9] A. H. Hoang, Phys. Rev. D **69**, 034009 (2004) [arXiv:hep-ph/0307376].

- [10] M. Beneke, Y. Kiyo and K. Schuller, Nucl. Phys. B **714** (2005) 67 [arXiv:hep-ph/0501289].
- [11] M. Beneke, Y. Kiyo and K. Schuller, Phys. Lett. B **658** (2008) 222 [arXiv:0705.4518 [hep-ph]].
- [12] A. A. Penin, A. Pineda, V. A. Smirnov and M. Steinhauser, Nucl. Phys. B **699**, 183 (2004) [arXiv:hep-ph/0406175].
- [13] A. Czarnecki and K. Melnikov, Phys. Lett. B **519**, 212 (2001) [arXiv:hep-ph/0109054].
- [14] S. Recksiegel and Y. Sumino, Phys. Rev. D **65**, 054018 (2002).
- [15] A. Pineda, J. Phys. G **29**, 371 (2003).
- [16] T. Lee, Phys. Rev. D **67**, 014020 (2003).
- [17] N. Brambilla, A. Vairo, X. Garcia i Tormo and J. Soto, Phys. Rev. D **80**, 034016 (2009) [arXiv:0906.1390 [hep-ph]].
- [18] G.T. Bodwin, E. Braaten, and G.P. Lepage, Phys. Rev. D 51 (1995) 1125; Erratum *ibid.* 55 (1997) 5853.
- [19] G. Källen and A. Sarby, K. Dan. Vidensk. Selsk. Mat.-Fis. Medd. 29, N17 (1955) 1.
- [20] A. Czarnecki and K. Melnikov, Phys. Rev. Lett. 80 (1998) 2531.
- [21] M. Beneke, A. Signer, and V.A. Smirnov, Phys. Rev. Lett. 80 (1998) 2535.
- [22] I. Harris and L.M. Brown, Phys. Rev. 105 (1957) 1656.
- [23] A. Czarnecki and K. Melnikov, Phys. Rev. D 65 (2002) 051501; Phys. Lett. B 519 (2001) 212.
- [24] B.A. Kniehl and A.A. Penin, Nucl. Phys. B 563 (1999) 200.
- [25] N. Brambilla, A. Pineda, J. Soto, and A. Vairo, Nucl. Phys. B 566 (2000) 275.
- [26] M. Beneke, Y. Kiyo and A. A. Penin, Phys. Lett. B **653** (2007) 53 [arXiv:0706.2733 [hep-ph]];
- [27] M. Beneke and Y. Kiyo, Phys. Lett. B **668** (2008) 143 [arXiv:0804.4004 [hep-ph]].
- [28] M. J. Strassler and M. E. Peskin, Phys. Rev. D **43** (1991) 1500.

- [29] K. Melnikov and A. Yelkhovsky, Nucl. Phys. B **528**, 59 (1998) [arXiv:hep-ph/9802379].
- [30] W. Fischler, Nucl. Phys. **B129**, 157 (1977);
B.A. Kniehl, A.A. Penin, V.A. Smirnov and M. Steinhauser, Phys. Rev. **D65**, 091503 (2002).
- [31] Y. Schroder, Phys. Lett. B **447**, 321 (1999) [arXiv:hep-ph/9812205];
M. Peter, Phys. Rev. Lett. **78**, 602 (1997) [arXiv:hep-ph/9610209].
- [32] N. Brambilla, A. Pineda, J. Soto and A. Vairo, Phys. Rev. D **60**, 091502 (1999).
- [33] B. A. Kniehl and A. A. Penin, Nucl. Phys. B **563**, 200 (1999).
- [34] A. Pineda and J. Soto, Phys. Lett. B **495**, 323 (2000).
- [35] C. Anzai, Y. Kiyo and Y. Sumino, arXiv:0911.4335 [hep-ph].
- [36] A. V. Smirnov, V. A. Smirnov and M. Steinhauser, arXiv:0911.4742 [hep-ph].
- [37] A. Pineda and A. Signer, Phys. Rev. D **73** (2006) 111501 [arXiv:hep-ph/0601185].
- [38] A. Signer, Phys. Lett. B **672** (2009) 333 [arXiv:0810.1152 [hep-ph]].
- [39] M. Beneke, Phys. Lett. B **434**, 115 (1998) [arXiv:hep-ph/9804241].
- [40] A. Pineda, JHEP **0106**, 022 (2001) [arXiv:hep-ph/0105008].
- [41] C. Amsler *et al.* [Particle Data Group], Phys. Lett. B **667**, 1 (2008).